CHEMISTRY & SUSTAINABILITY
CHEMSUSCHEM
ENERGY & MATERIALS

Supporting Information

A Visible-Light Harvesting System for CO_2 Reduction Using a Ru^{II}–Re^{I} Photocatalyst Adsorbed in Mesoporous Organosilica

Yutaro Ueda,[a] Hiroyuki Takeda,[a] Tatsuto Yui,[c] Kazuhide Koike,[d] Yasutomo Goto,[b] Shinji Inagaki,*[b] and Osamu Ishitani*[a]

cssc_201403194_sm_miscellaneous_information.pdf

Contents

I. Experimental Details

Materials

Acetonitrile (MeCN) was dried over P_2O_5 three times and then distilled from CaH_2 prior to use. DMF and triethanolamine (TEOA) was distilled under reduced pressure. They were kept under Ar atmosphere prior to use. Other reagents and solvents were commercial-grade quality and used without further purification.

Syntheses

1,2-bis(4'-methyl-[2,2'-bipyridine]-4-yl)ethane (**BL**);[1] 4,4'-bis(diethylmethylphosphonate)-2,2'-bipyridine (**L2**);[2] $[Ru(dmb)_2(L1)](PF_6)_2$ (**Ru**, L1 = 4,4'-bis(methyl-phosphonate)-2,2'-bipyridine);[2] $[Ru(dmb)(L2)(BL)](PF_6)_2$;[3] 1,3-dimethyl- 2-phenylbenzimidazoline (BIH);[4] **MCM–41**;[5] as-made **Acd–PMO**;[6] and 2,7-bis(triethoxysilyl)-9-methylacridone (BTEMeAcd)[7] were synthesized according to previous procedures.

$[(dmb)(L2)Ru(BL)Re(CO)_3Br](PF_6)_2$ (Ru–Re)

$[Ru(dmb)(L2)(BL)](PF_6)_2$ (63.4 mg, 0.045 mmol) and $Re(CO)_5Br$ (19.0 mg, 0.047 mmol) were dissolved in EtOH/Acetone (1:1) mixed solution (40 mL). The solution was refluxed for 3 h under N_2 atmosphere. After the solvent was evaporated, the residue was subjected to column chromatography on SP Sephadex C-25, using a 1:1 mixture of acetone‐water containing NH_4PF_6 as an eluent. The product was recrystallized from methylenechloride-ether.

Yield: 51.2 mg (0.021 mmol, 70%)

^{1}H NMR (acetone-d_6, 400 MHz) : δ/ppm : 8.95 (m, 2H), 8.50-8.36 (m, 8H), 7.72-7.25 (m, 14H), 4.15-4.06 (m, 8H, -POCH_2CH$_3$), 3.50 (d, 4H, -CH_2PO$_3$Et$_2$), 3.38-3.34 (m, 4H, -CH_2CH_2-), 2.68-2.57 (m, 12H, py-CH_3), 1.29-1.22 (m, 12H, -POCH$_2$CH_3).

ESI-MS (MeCN): 729, $[M–2(PF_6)]^{2+}$.

FT-IR (MeCN): 1899, 1917, and 2022 cm^{-1}.

Anal. Calculated for $C_{94}H_{88}F_{24}N_8O_8P_7ReRu$: C, 40.53; H, 3.69; N, 6.41. Found: C, 40.27; H, 3.61; N, 6.18

$[(dmb)(L1)Ru(BL)Re(CO)_3Br](PF_6)_2$ (Ru–Re)

$[(dmb)(L2)Ru(BL)Re(CO)_3Br](PF_6)_2$ (32.5 mg, 0.013 mmol) and TMS-Br (0.2 ml) were dissolved in MeCN (10 mL) and the solution was stirred at 60 °C for 12 h under N_2 atmosphere. The reaction was quenched by methanol addition and the solvent was evaporated. The residue was dissolved in methanol, and after addition of a saturated NH_4PF_6 solution, the mixture was concentrated by evaporation. Precipitated solids were filtered and dried in vacuo.

Yield: 20.2 mg (0.0088 mmol, 67%)

FT-IR (MeCN): 1899, 1917, and 2022 cm^{-1}.

^{31}P NMR (159 MHz, MeCN): δ/ppm 23.52 (-PO_3H_2), −139.56(PF_6).

Anal. Calculated for $C_{51}H_{48}BrF_{12}N_8O_9P_4ReRu$: C, 37.44; H, 2.96; and N, 6.85. Found: C, 37.55; H, 3.25; and N, 6.95.

UV-vis Abs.: λ_{max} (MLCT) = 460 nm (ε = 16,300 $M^{-1}cm^{-1}$).

Acd–PMO

As-made material of **Acd-PMO** was heated under a tetraethyl orthosilicate atmosphere at 120°C overnight. The obtained powder was washed with ethanol several times and stirred in a 9:1 $NaHCO_3$ (0.1 M) and $NaCO_3$ (0.05 M) mixed aqueous solution (v/v, pH 8.9) at room temperature for 24 h. The pH of the obtained suspension was adjusted to 7 by addition of an aqueous HCl solution and then the dispersion was added to ethanol and stirred at room temperature overnight. The precipitated solids were collected by filtration and dried at room temperature.

MeAcd–PMO

Docosyltrimethylammonium chloride (C_{22}TMACl, 4.5 g) was dissolved in a mixture of water (900 g), EtOH (540 g), and ammonia solution (15 mL, 28 wt%). An ethanolic solution (2.6 mL) containing BTEMeAcd (0.115 g/mL) was added dropwise to the mixture with vigorously stirring. The reaction was allowed to proceed for 24 h at room temperature under stirring and the precipitated solids were collected by filtration and dried at room temperature. The solid (0.5 g) was added to ethanol (100 mL) containing 2 M hydrochloric acid (1 mL) and stirred overnight at room temperature for surfactant removal.

Adsorption of Ru–Re in Acd–PMO

Acd–PMO (5–30 mg) was added to a MeCN solution (15 mL) containing **Ru–Re** (0.01–10 μmol) and the suspension was stirred overnight at room temperature in the dark. The hybrid material **Ru–Re/Acd–PMO** was isolated by filtration and washed with MeCN. The UV-vis absorbance of filtrate and MeCN wash was measured at 460 nm to determine the **Ru–Re** loading (ε_{460nm} = 16,300 $M^{-1}cm^{-1}$).

General Measurements

^{1}H NMR and ^{31}P NMR were measured using a JEOL AL300, AL400, or ECX400 system. Electrospray ionization-mass spectroscopy (ESI-MS) was performed with a Shimadzu LCMS-2010A system using MeCN as a mobile phase. UV-vis absorption spectra were measured using a JASCO V-565 spectrophotometer, which was equipped with an integral sphere unit for diffuse reflectance measurements, and $BaSO_4$ was used as a standard. FT-IR spectra were acquired in MeCN or KBr pellets using a JASCO FT/IR-610 spectrometer.

Emission spectra and emission quantum yields were recorded using an absolute photoluminescence quantum yield measurement system (Hamamatsu photonics, C9920-01, 02). The emission quantum yields

of acridone, **Ru**, and **Re** units in **Ru–Re/Acd–PMO** were determined by global fitting analysis of the summation spectra of the model compounds **Acd–PMO**, **Ru/MCM–41(I)**, and **Re/MCM–41(I)**, respectively, using a non-linear least square curve fitting method. Emission spectral shapes resulting from direct excitation were utilized as model emission spectra for spectral fitting. A typical example of the fitting is shown in Figure S6.

Emission lifetimes were measured using a HORIBA Jobin Yvon FluoroCube time-correlated single-photon counting system equipped with a NanoLED-405L (λ_{max} = 401 nm) as an excitation light-source. The instrument response was less than 200 ps. Samples were dispersed in MeCN (*ca*. 0.05 mg mL^{-1}) by sonication and purged with Ar for 30 min before emission measurements.

Powder X-ray diffraction (XRD) patterns were acquired using a MiniFlex600 instrument equipped with a CuKα X-ray source (Rigaku). Nitrogen adsorption/desorption measurements were conducted at 77 K using a BELLSORP-miniII analyzer (Bell Japan). The Brunauer–Emmett–Teller (BET) surface area was calculated using adsorption data for relative pressures ranging from 0.08 to 0.2. Pore size distributions were calculated using the density functional theory (DFT) method (DFT kernel: N_2 at 77 K on silica, cylindrical pores, nonlinear density functional theory (NLDFT) equilibrium model). Pore volumes were calculated from adsorption branches of isotherms using the t-formula.

Calculation of the absorbed and emitted photons by Ru–Re/Acd–PMO

Assuming a homogeneous dispersion of each component, i.e., **Acd** units and **Ru–Re**, in an MeCN solution, the contributions of **Acd** units and **Ru–Re** to light absorption ($A_{\mathbf{Acd}}$ and $A_{\mathbf{Ru–Re}}$) were estimated using the molar extinction coefficient and the number of each component. The measured molar extinction coefficient of the **Acd–PMO** precursor 2,7-bis(triethoxysilyl)acridone (ε_{405nm}(**Acd**)) equaled 1.9×10^3 M^{-1} cm^{-1} in 2-propanol. The measured molar extinction coefficient of **Ru–Re** (ε_{405nm}(**Ru–Re**)) amounted to 1.0×10^4 M^{-1} cm^{-1} in MeCN. The number of **Acd** units in the dispersion was calculated using the formula weight of **Acd–PMO** ($_{1.5}$OSi–$C_{13}H_9NO$–$SiO_{1.5}$: 299.39 g mol^{-1}). For example, even at the highest adsorbed amount (93 μmol g^{-1}), $A_{\mathbf{Acd}}$ and $A_{\mathbf{Ru–Re}}$ equaled 0.88 and 0.12, respectively.

The total numbers of photons absorbed (n_{abs}(total)) and emitted by **Ru–Re/Acd–PMO** (n_{em}(total)) during emission measurements were counted using an absolute emission quantum yield measurement system and an integral sphere.[8] The number of absorbed photons by each component were estimated using the following equations.

$$n_{abs}(\mathbf{Acd}) = n_{abs}(\text{total}) \times A_{\mathbf{Acd}} \qquad \text{(S1)}$$

$$n_{abs}(\mathbf{Ru–Re}) = n_{abs}(\text{total}) \times A_{\mathbf{Ru–Re}} \qquad \text{(S2)}$$

$$A_{\mathbf{Acd}} + A_{\mathbf{Ru–Re}} = 1 \qquad \text{(S3)}$$

The total number of photons emitted by **Ru–Re/Acd–PMO** (n_{em}(total)) was divided into emission contributions for each component (n_{em}(**Acd**) and n_{em}(**Ru**-total)) by global fitting analysis of the emission

spectra of **Ru–Re/Acd–PMO** (Figure S10), and the total number of photons emitted by **Ru–Re** in the hybrid (n_{em}(**Ru**-total)) was divided into excitation contributions for **Acd** and **Ru–Re** units (Scheme S1). For direct excitation of **Ru–Re** units, the number of photons emitted by Ru units (n_{em}'(**Ru**)) was calculated using the emission quantum yield of **Ru–Re/Acd–PMO** under excitation at 460 nm ($\Phi_{Ru–Re}$ = 0.109) (eq. (S4)). On the other hand, the number of photons emitted by Ru units via energy transfer from **Acd** to Ru units (n_{em}(**Ru**)) was estimated by substrating n_{em}'(**Ru**) from n_{em}(**Ru**-total) (eq. (S5)).

$$n_{em}'(\mathbf{Ru}) = n_{abs}(\mathbf{Ru–Re}) \times \Phi_{Ru–Re} \qquad (S4)$$

$$n_{em}(\mathbf{Ru}) = n_{em}(\mathbf{Ru}\text{-total}) - n_{em}'(\mathbf{Ru}) \qquad (S5)$$

These calculated values provided quantum yields for the emission of the excited Ru units produced via energy transfer from the **Acd** units (Φ_{hybrid}(**Ru**)) using eq. (1), as described in the main manuscript.

$$\Phi_{hybrid}(\mathbf{Ru}) = n_{em}(\mathbf{Ru})/n_{abs}(\mathbf{Acd}) \qquad (1)$$

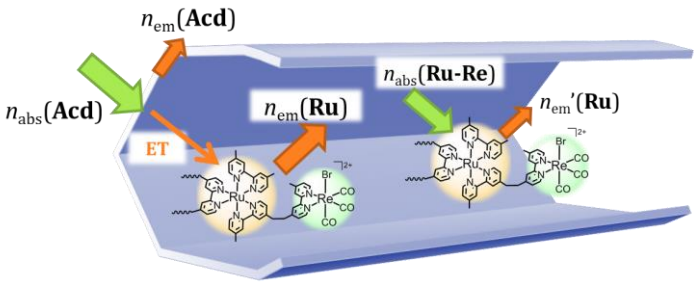

Scheme S1. Photophysical processes involved in the excited state of **Ru–Re/Acd–PMO** via excitation of **Acd** or Ru units.

Under photocatalytic CO_2 reduction conditions, if **Ru–Re/Acd–PMO** absorbs 100 photons at 405 nm, **Acd** groups and **Ru–Re** absorb 96 and 4 photons, respectively. Because the energy transfer from the excited **Acd** groups to the Ru units occurs at 80% efficiency, 77 Ru units are excited by the energy transfer, meaning that 85 excited Ru units are produced overall. On the other hand, only 8 irradiated photons are absorbed by **Ru–Re/MCM–41(I)** under the same irradiation conditions. Therefore, the number of excited Ru units should be about ten-fold larger in **Ru–Re/Acd–PMO** than in **Ru–Re/MCM–41(I)** under these conditions.

Photocatalytic reactions

The hybrid material (1 mg) was dispersed in a DMF–TEOA (5:1 v/v, 4 ml) mixed solution containing BIH (0.1 M). The suspension was introduced in an 11-ml pyrex-glass tube and gently bubbled with CO_2 for 30 min. The suspension was irradiated at 405 nm using a 500 W high-pressure mercury lamp and solution filters comprising 1% $NaNO_2$ in H_2O (w/v) and 0.75% I_2 in CCl_4 (w/v). The reactor was cooled using tap

water during the irradiation. Gaseous products (CO, H_2) were analyzed using a GC-TCD instrument (GL science GC323) equipped with an active carbon column. The liquid product HCOOH was analyzed using a capillary electrophoresis system (Otsuka Electronics Co. CAPI–3300).

II. Figures

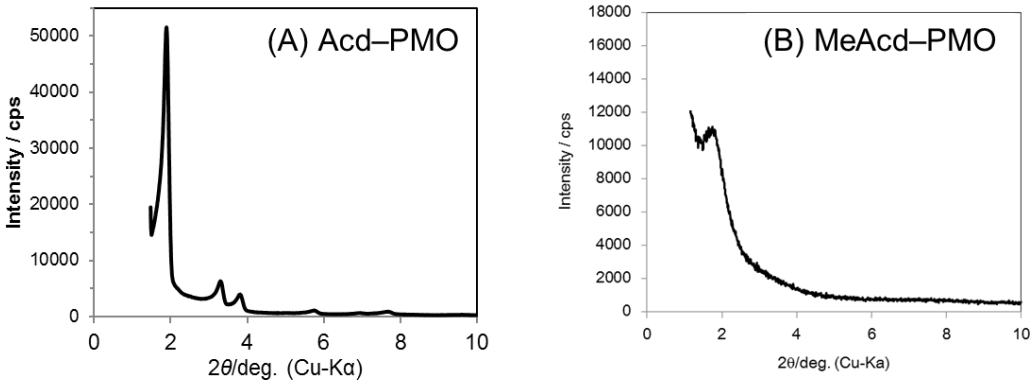

Figure S1. Powder XRD patterns of (A)**Acd–PMO** and (B)**MeAcd–PMO**.

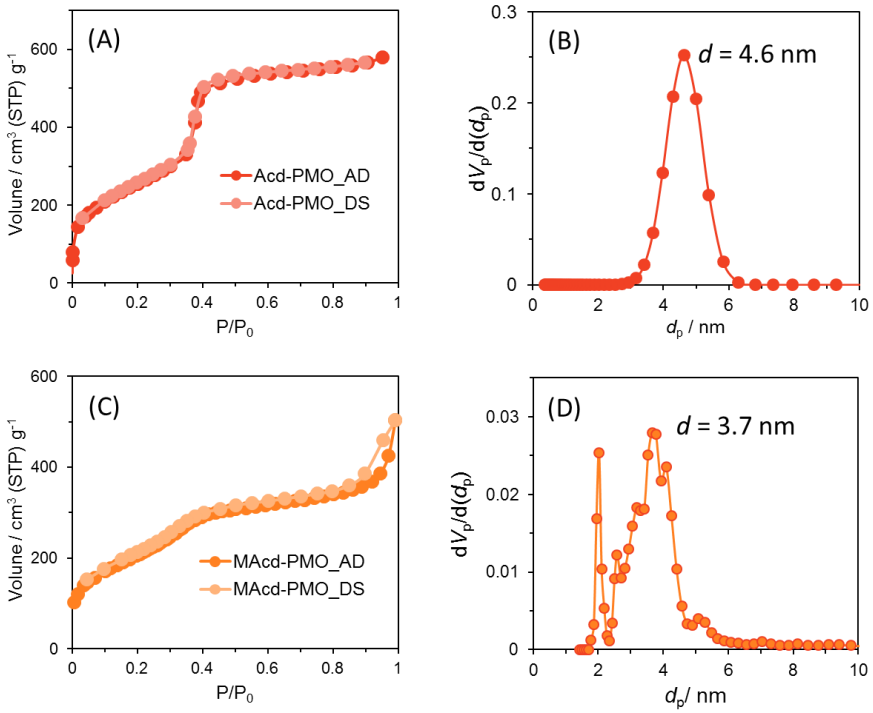

Figure S2. Nitrogen adsorption/desorption isotherms and pore-size distributions of **Acd–PMO** (A, B) and **MeAcd–PMO** (C, D).

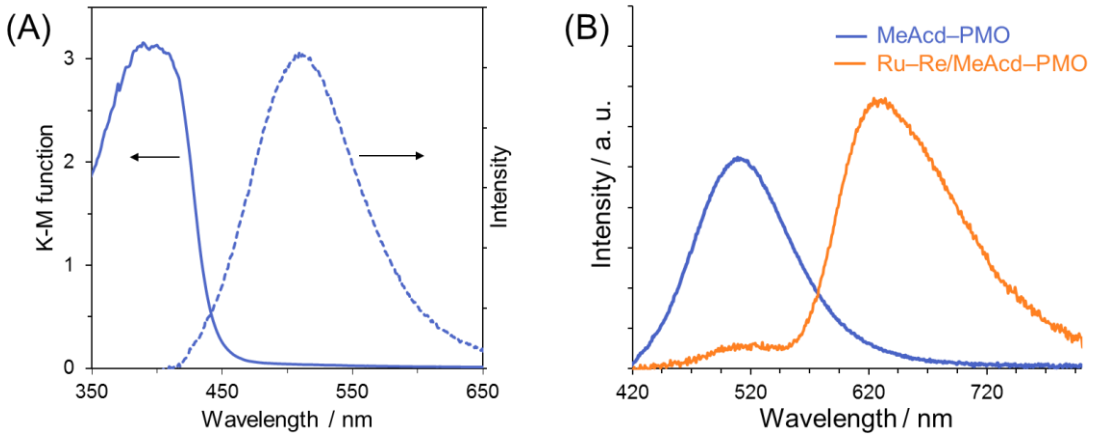

Figure S3. (A) UV-vis DR and emission spectra of **MeAcd–PMO**. (B) Emission spectral change of **MeAcd–PMO** by adsorption of **Ru–Re** (54 μmol g^{-1}, [**Ru–Re**]/[**MeAcd**] = mol%). (Emission spectrum was measured in MeCN dispersion and emission intensities were normalized by the absorbance at the excitation wavelength the excitation wavelength at 405 nm.)

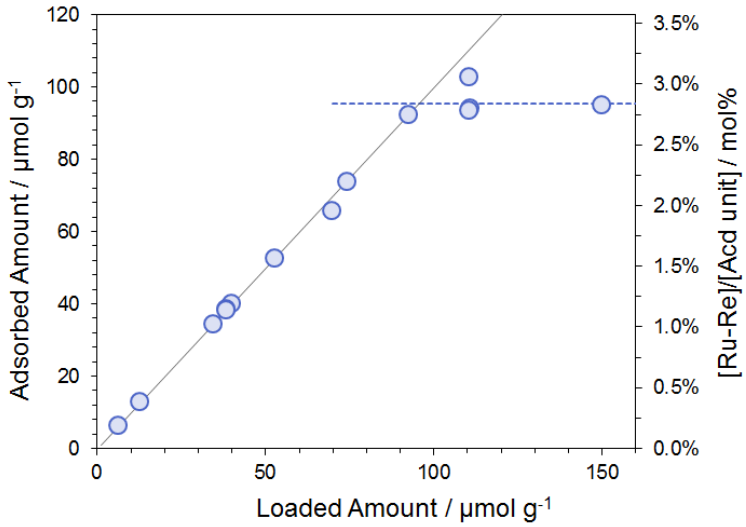

Figure S4. Relationship between **Ru–Re** loadings in solution and in **Acd–PMO**.

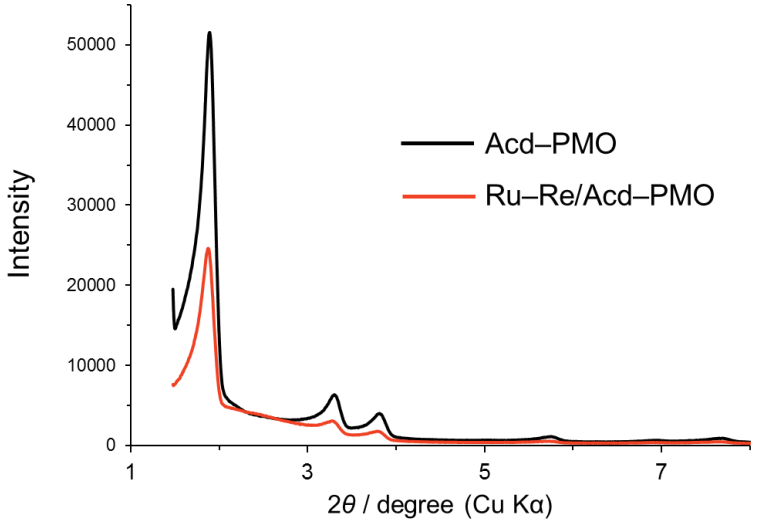

Figure S5. Powder XRD patterns of **Acd–PMO** and **Ru–Re/Acd–PMO**.

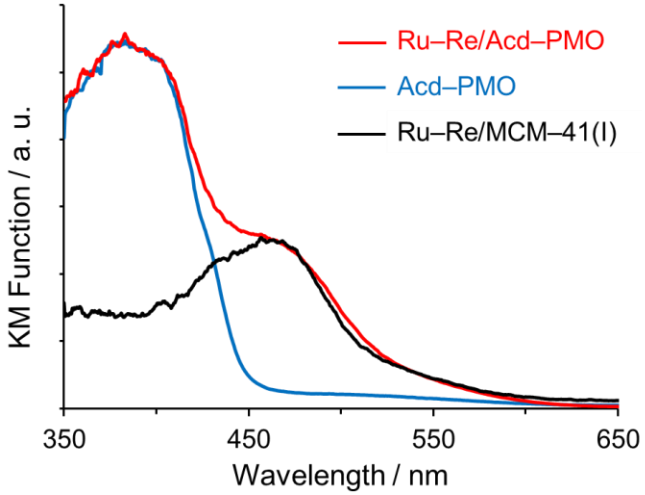

Figure S6. UV-vis DR spectra of **Ru–Re/Acd–PMO** (red line), **Acd–PMO** (blue line), and **Ru–Re/MCM–41(I)** (black line).

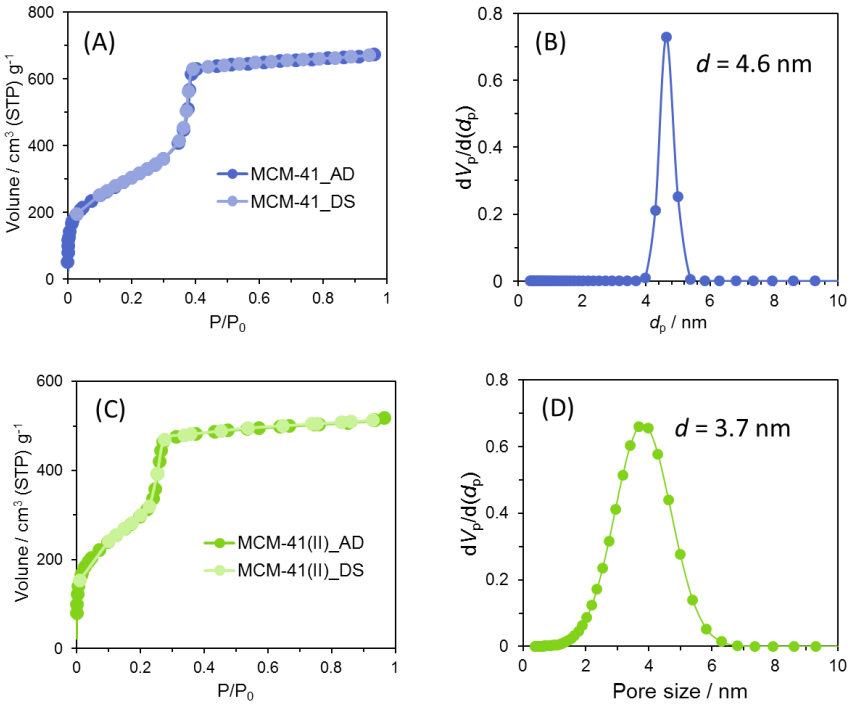

Figure S7. Nitrogen adsorption/desorption isotherms and pore-size distributions of **MCM–41(I)** (A, B) and **MCM–41(II)** (C, D).

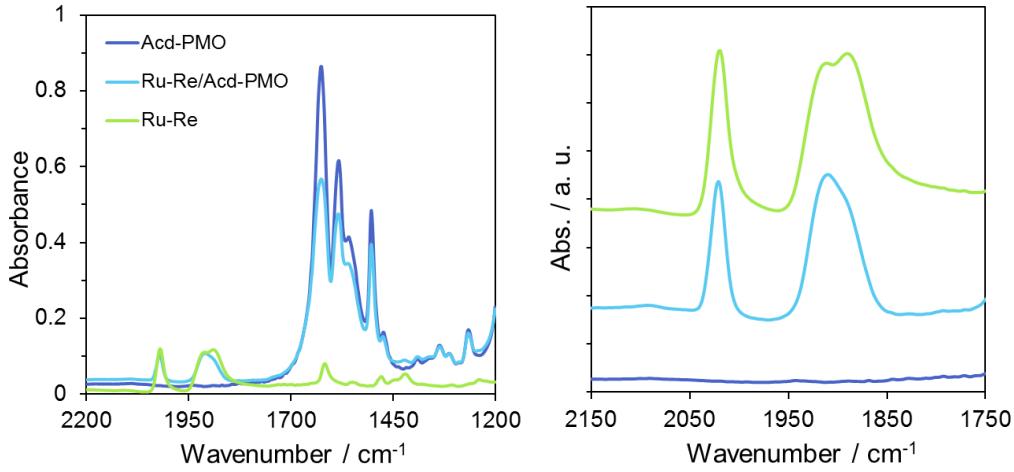

Figure S8. FT-IR spectra of **Acd–PMO**, **Ru–Re/Acd–PMO**, and **Ru–Re** in KBr pellets.

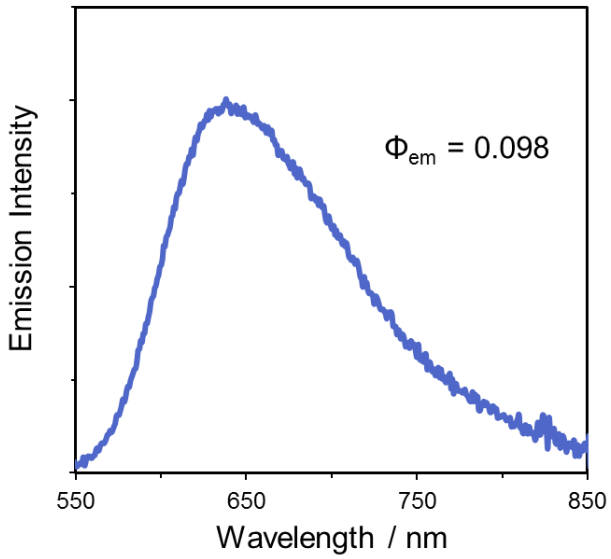

Figure S9. Emission spectrum of **Ru–Re/MCM–41(I)** at an excitation wavelength of 456 nm.

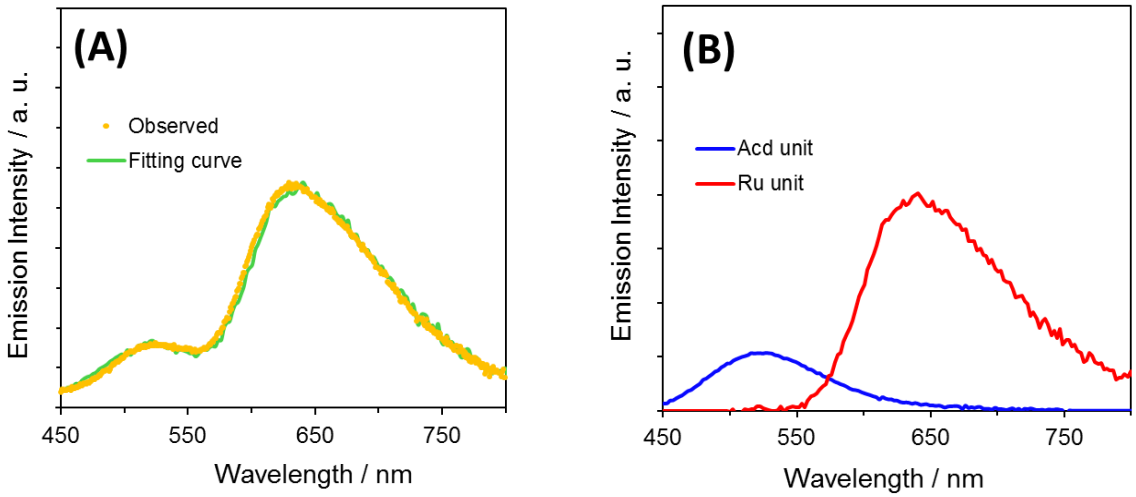

Figure S10. (A) Observed emission spectrum and fitting curve simulated by global fitting analysis for the **Ru–Re/Acd–PMO** (40 μmol g^{-1}). (B) Emission spectra of each Acd units and Ru units of **Ru–Re/Acd–PMO** (40 μmol g^{-1}). [Note] There was no contribution of the emission from Re units.

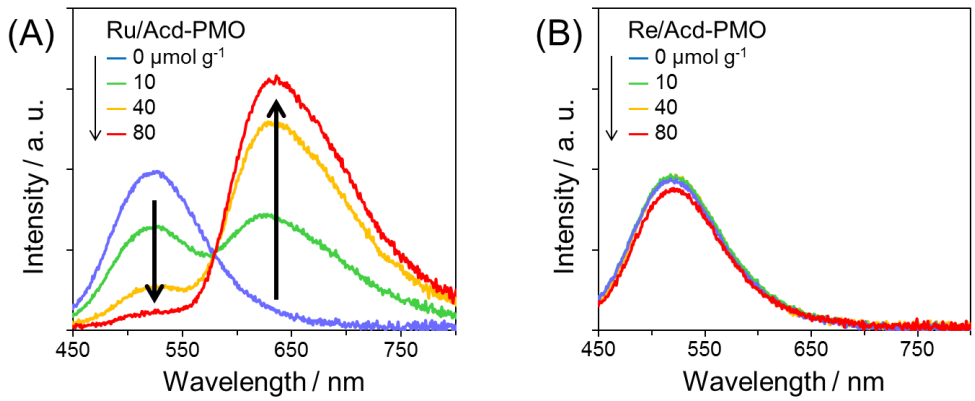

Figure S11. Changes in the emission spectra of (A) **Ru/Acd–PMO** and (B) **Re/Acd–PMO** for various adsorbed amounts of metal complexes.

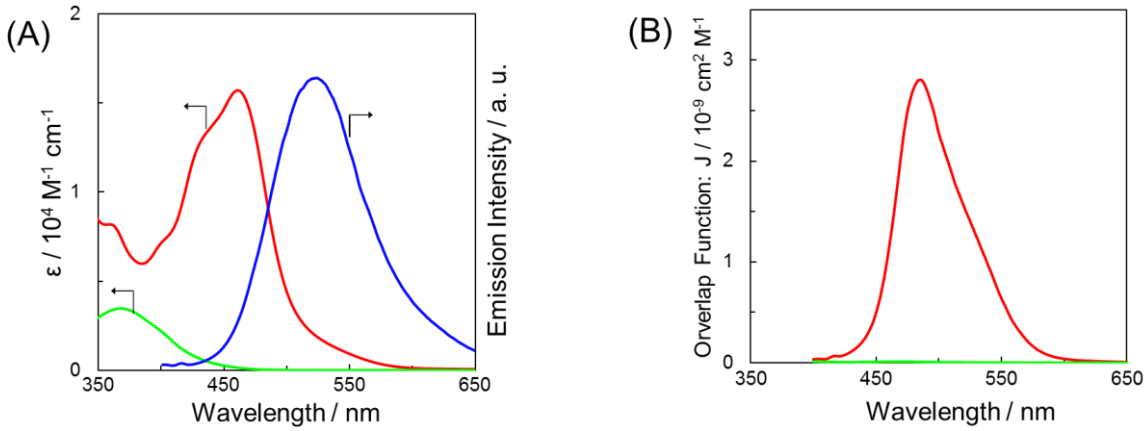

Figure S12. (A) Emission spectrum $F_D(\lambda)$ of **Acd–PMO** (blue line) and absorption spectra $\varepsilon_A(\lambda)$ of **Ru** (red) and **Re** (green). (B) Spectral overlaps between the emission spectrum of **Acd–PMO** and the extinction spectra of **Ru** (red) and **Re** (green). The overlap functions ($J(\lambda)$) were calculated using $J(\lambda) = \lambda^4 \times F_D(\lambda)\ \varepsilon_A(\lambda)$.

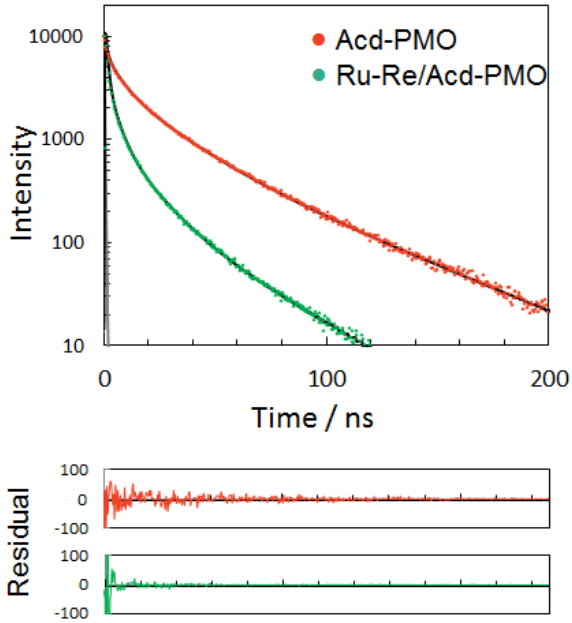

Figure S13. Emission decay profiles of **Acd–PMO** and **Ru–Re/Acd–PMO** (63 μmol g^{-1}) observed at 500 nm (excitation wavelength: 401 nm).

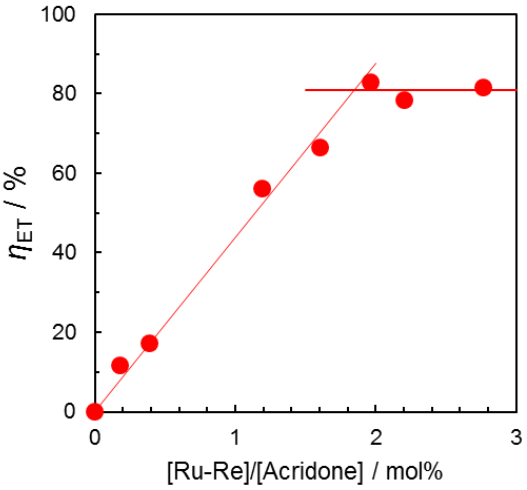

Figure S14. Energy transfer efficiency (η_{ET}) from the excited **Acd** groups to Ru units in **Ru–Re/Acd–PMO** for different **Ru–Re** loadings.

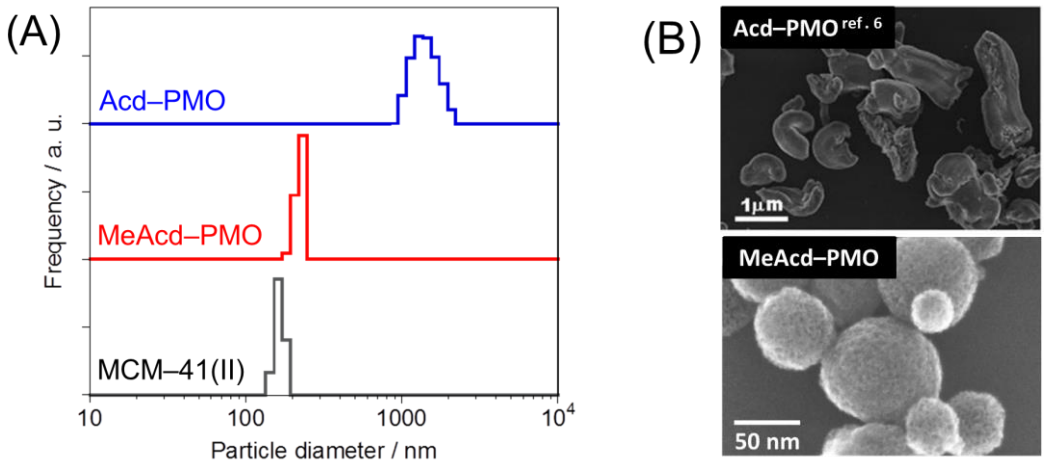

Figure S15. (A) Particle size distributions of **Acd–PMO**, **MeAcd–PMO**, and **MCM–41(II)** dispersed in a 5:1 DMF–TEOA (v/v) mixture measured by dynamic light scattering. (B) SEM images of **Acd–PMO**[6] (Reproduced by permission of The Royal Society of Chemistry) and **MeAcd–PMO**.

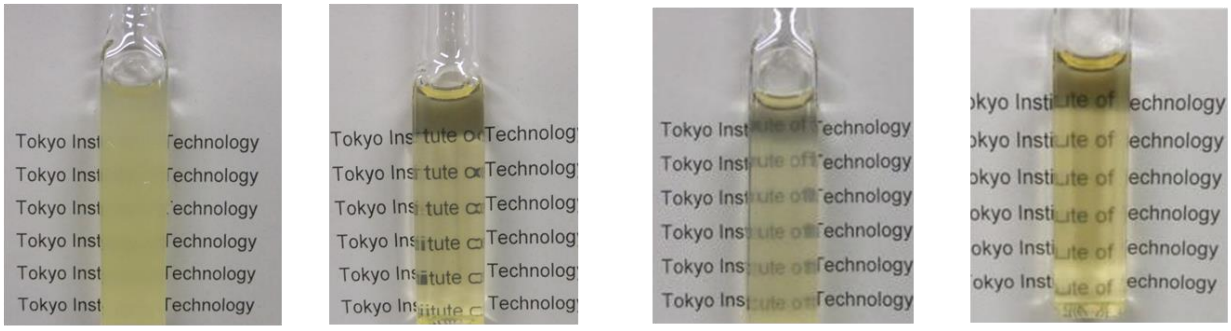

Figure S16. Photographs of the hybrids dispersed in a 5:1 DMF–TEOA (v/v) mixture.

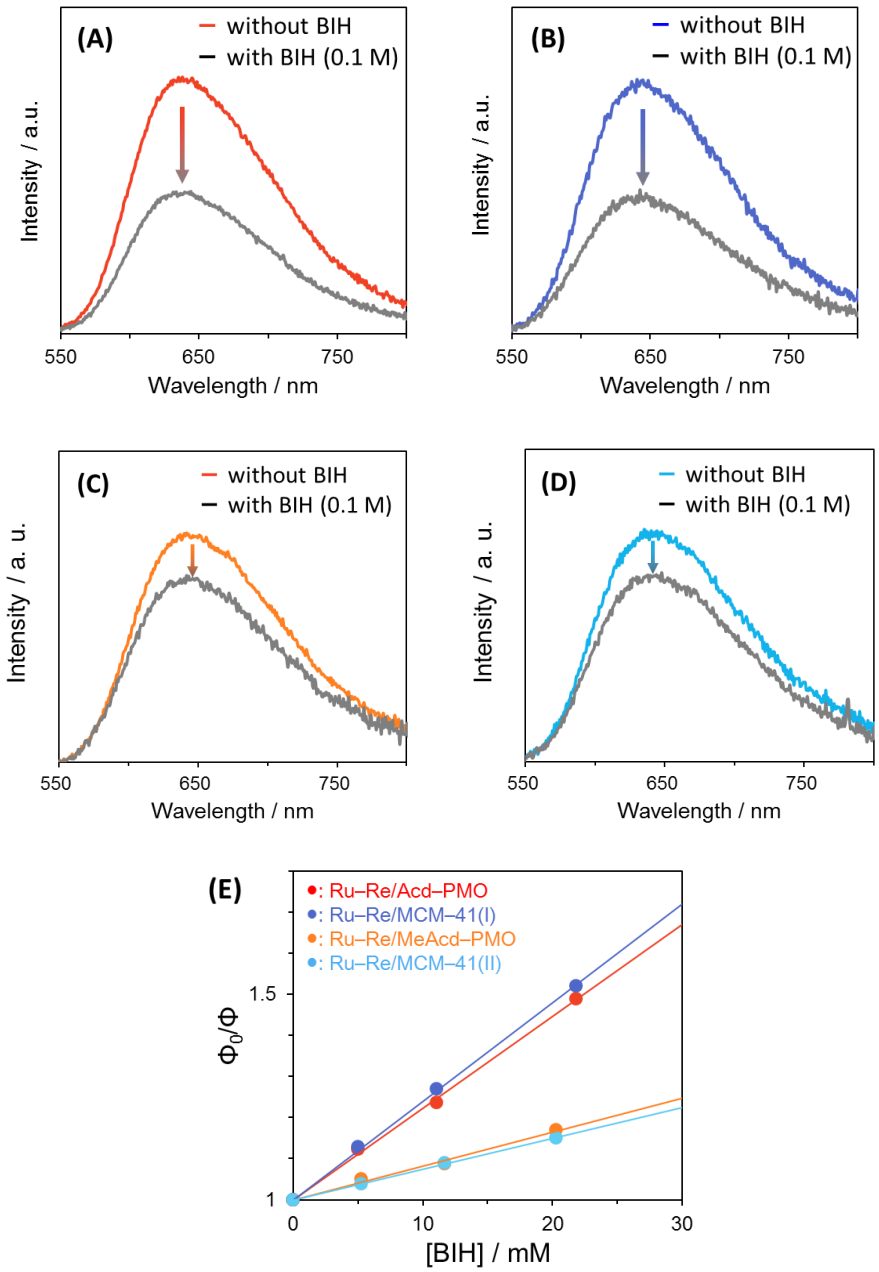

Figure S17. Emission spectra of (A) **Ru–Re/Acd–PMO** (63 μmol g^{-1}), (B) **Ru–Re/MCM–41(I)** (64 μmol g^{-1}), (C) **Ru–Re/MeAcd–PMO** (54 μmol g^{-1}), and (D) **Ru–Re/MCM–41(II)** (57 μmol g^{-1}) in the absence and presence of BIH (0.1 M) in 5:1 DMF–TEOA (v/v) dispersions (excitation wavelength: 405 nm). (E) Stern–Volmer plots for emission quenching of **Ru–Re** in the hybrids using BIH as a reductant (Φ_0: emission quantum yield in the absence of BIH and Φ: in the presence of BIH).

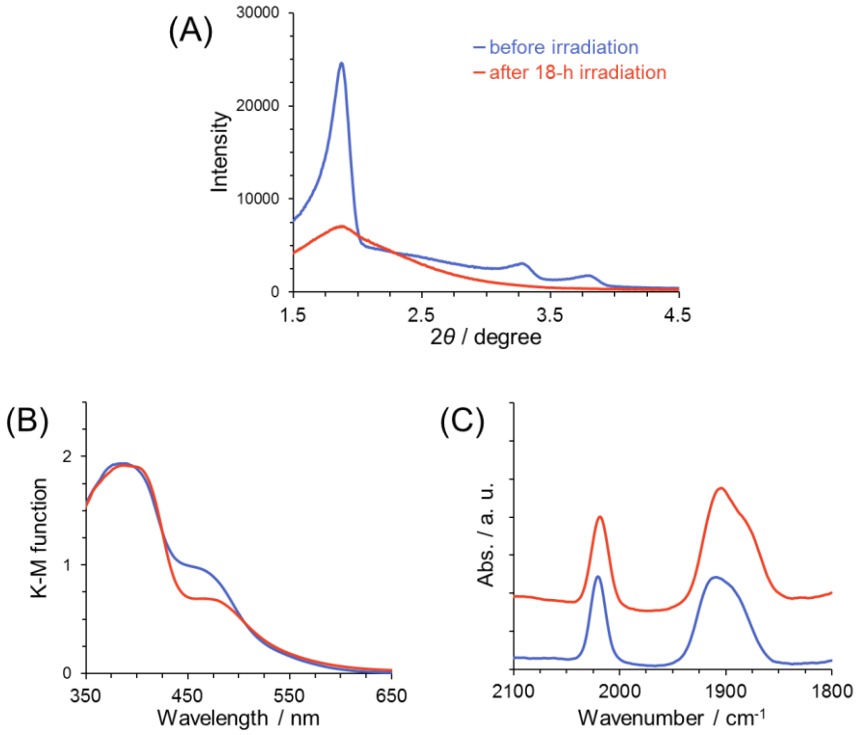

Figure S18. (A) Powder XRD patterns, (B) UV-vis DR spectra, and (C) FT-IR spectra (in KBr pellet) of **Ru–Re/Acd–PMO** before (blue line) and after 18-h irradiation (red line).

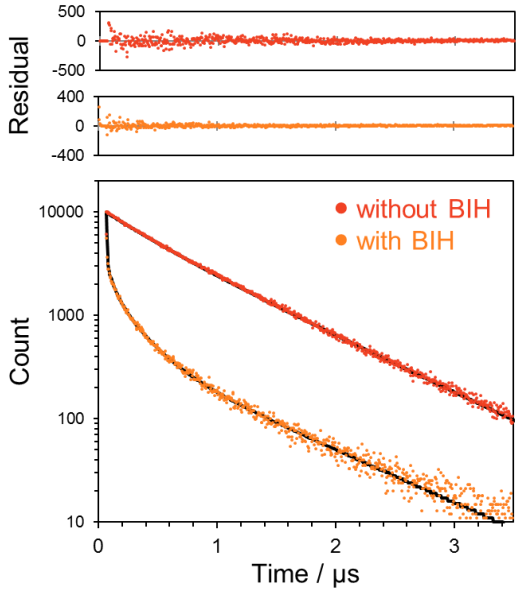

Figure S19. Emission decays from the Ru unit in **Ru–Re/Acd–PMO** in the absence of 0.1 M of BIH (red) and in the absence of BIH (orange) (λ_{ex} = 456 nm, λ_{obs} = 700 nm). These can be fitted with multi-exponential functions and the obtained lifetimes of emission were as follows: without BIH, τ_{em} = 787 ns (92%) and 382 ns (8%); with BIH, 779 ns (7%), τ_{em} = 342 ns (12%), 94 ns (27%), and 7 ns (54%)

III. Tables

Table S1. Emission quantum yields and energy transfer efficiencies of **Ru–Re/Acd–PMO** for various **Ru–Re** loadings in MeCN dispersions. For each component, emission quantum yields (Φ_{hybrid}(**Acd**), Φ_{hybrid}(**Re**), and Φ_{hybrid}(**Ru**)) were obtained by a global fitting analysis of the emission spectra of hybrid materials excited at 405 nm.

$[Ru–Re]_{Ads}$ [a]	[Ru–Re]/[Acd]	Emission quantum yield			η_{ET} / % [b]	N [c]
μmol g^{-1}	mol%	Φ_{hybrid}(Acd)	Φ_{hybrid}(Ru)	Φ_{hybrid}(Re)		
0	0	0.029	-	-	0	-
6	0.2	0.024	0.012	0	12	66
13	0.4	0.021	0.018	0	17	45
40	1.2	0.013	0.058	0	56	47
53	1.6	0.008	0.065	0	66	42
66	2.0	0.003	0.086	0	83	42
74	2.2	0.004	0.074	0	78	36
93	2.8	0.003	0.070	0	82	29

[a]Amount of adsorbed **Ru–Re** molecule in 1 g of **Acd–PMO**. [b]Energy transfer efficiency from the excited state of Acd-units to **Ru–Re** complexes. [c]Number of Acd units that transferred the excitation energy to one **Ru–Re** molecule.

Table S2. Emission Lifetime [a]

	λ_{ex} / nm	λ_{obs} / nm	τ_1 / ns	τ_2 / ns	τ_3 / ns	τ_4 / ns
Acd–PMO	401	500	1.0 (21%)	5.7 (36%)	21.2 (32%)	52.2 (12%)
Ru–Re/Acd–PMO [b]	401	500	0.7 (46%)	3.1 (37%)	11.9 (15%)	36.4 (3%)
Ru–Re/Acd–PMO	401	700	816 (94%)	369 (6%)	-	-
Ru–Re/Acd–PMO	456	700	787 (92%)	382 (8%)	-	-
Ru/MCM–41(I)	456	700	853 (92%)	411 (8%)	-	-
Ru–Re/Acd–PMO [c]	456	700	779 (7%)	342 (12%)	94 (27%)	7 (54%)

[a]The excitation wavelength was 401 nm for **Acd–PMO** excitation, and 456 nm for **Ru–Re** excitation. The lifetimes were observed at 500 nm for the emission from **Acd–PMO**, and 700 nm for the emission from **Ru–Re**. [b]Amount of **Ru–Re** adsorbed in **Acd–PMO**: 63 μmol g^{-1}. [c]In the presence of BIH (0.1 M).

Table S3. Control Experiments for Photocatalytic CO_2 Reduction

Photocatalyst	$[MC]_{Ads}$/μmol g^{-1}	TON_{CO} [a]	TON_{H2} [a]	Note
Ru–Re/Acd–PMO	64	611 (39 μmol)	10 (0.6 μmol)	Entry 1 in Table 2
Ru–Re/Acd–PMO	64	0	0	In the dark
Ru–Re/Acd–PMO	64	0	0	Under Ar
Ru–Re/Acd–PMO	64	0	0	Without BIH
Acd–PMO	0	(0 μmol)	(0.3 μmol)	Without **Ru–Re**
Ru/Acd–PMO	66	2	12	Without **Re**
Re/Acd–PMO	66	13	15	Without **Ru**

[a]The turnover number was calculated based on the metal complex used.

Table S4. Reductive Quenching of Ru–Re in the Hybrids by BIH

hybrids	K_{SV} / M^{-1} [a]	η_q / % [b]
Ru–Re/Acd–PMO	22	45
Ru–Re/MCM–41(I)	24	43
Ru–Re/MeAcd–PMO	8.2	18
Ru–Re/ MCM–41(II)	7.5	17

[a]The Stern-Volmer constants obtained from the Stern–Volmer plots (Figure S17(E)).

[b]Quenching efficiency of the emission from **Ru–Re** in the hybrids using 0.1 M of BIH.

IV. References

1. Christian Kaes, M. W. H., Andre De Cian, Jean Fischer, *Tetrahedron Lett.*, **1997**, *38*, 3901-3904.
2. Gillaizeau-Gauthier, I.; Odobel, F.; Alebbi, M.; Argazzi, R.; Costa, E.; Bignozzi, C. A.; Qu, P. and Meyer, G. J., *Inorg. Chem.*, **2001**, *40*, 6073-6079.
3. Freedman, D. A.; Evju, J. K.; Pomije, M. K. and Mann, K. R., *Inorg. Chem.*, **2001**, *40*, 5711-5715.
4. Hasegawa, E.; Seida, T.; Chiba, N.; Takahashi, T. and Ikeda, H., *J. Org. Chem.*, **2005**, *70*, 9632-9635.
5. Yokoi, T.; Yoshitake, H. and Tatsumi, T., *J. Mater. Chem.*, **2004**, *14*, 951.
6. Takeda, H.; Goto, Y.; Maegawa, Y.; Ohsuna, T.; Tani, T.; Matsumoto, K.; Shimada, T. and Inagaki, S., *Chem. Commun.*, **2009**, 6032-6034.
7. Maegawa, Y.; Mizoshita, N.; Tani, T. and Inagaki, S., *J. Mater. Chem.*, **2010**, *20*, 4399.
8. Suzuki, K.; Kobayashi, A.; Kaneko, S.; Takehira, K.; Yoshihara, T.; Ishida, H.; Shiina, Y.; Oishi, S.; Tobita, S., *PCCP*, **2009**, *11*, 9850.